Astron. Astrophys. 329, 776–784 (1998)

ASTRONOMY
AND
ASTROPHYSICS

Jovian decameter emissions observed by the Wind/WAVES radioastronomy experiment

A. Lecacheux[1], **M.Y. Boudjada**[2], **H.O. Rucker**[2], **J.L. Bougeret**[3], **R. Manning**[3], **and M.L. Kaiser**[4]

[1] CNRS-URA 1757, ARPEGES, Observatoire de Paris-Meudon, F-92195 Meudon, France
[2] Space Research Institute, A-8010 Graz, Austria
[3] CNRS-URA 264, DESPA, Observatoire de Paris-Meudon, F-92195 Meudon, France
[4] NASA / Goddard Space Flight Center, Greenbelt, MD 20771, USA

Received 2 January 1997 / Accepted 11 July 1997

Abstract. The WAVES radio astronomy experiment aboard the Wind spacecraft covers the frequency range from 1 MHz to 13.8 MHz with spectral resolution six times better than that of the Voyager PRA experiment. By combining Wind/WAVES observations with simultaneous observations made by the Nançay Decametric Array (France) between 10 and 40 MHz, the entire frequency spectrum of the jovian decametric emission can be observed. Two representative Io-controlled events (Io-B/D and Io-C) have been selected and analysed in terms of the available models of the jovian environment. In the case of the Io-B/D event at frequencies below 20 MHz, observations and models, to some extent, may fit an emission beam aperture of about 87°. To explain the higher frequencies we must assume that small refraction effects take place near the source region, consistent with topside jovian ionospheric parameters deduced from previous direct measurements. The Io-C event cannot be explained with this simple emission beam geometry: additional effects have to be invoked, as strong propagation effects near caustics or large distortion of the magnetic field in the source.

Key words: planets and satellites: Jupiter – radio continuum: solar system

1. Introduction

1.1. Ground-based observations

The Jovian decametric emission (DAM) is the most powerful radiation among our solar system planets. Ground-based observatories have been monitoring this planet since decades, since the discovery of this radiation in 1955 (Burke & Franklin, 1955). Observations of Jupiter with broadband spectrographs reveal that the emission pattern is principally organized as a function of the observer's position with respect to the planetary magnetic field (described by the central meridian longitude, CML), and sometimes of the orbital phase of Io Φ_{Io} (Bigg, 1964). The Io-dependent emissions are classified into components of radiation, labeled as "sources" A, B, C, and D. Dulk (1967) was the first author to suggest that the Jovian decametric radiation (in particular the Io-controlled part) was beamed into a "thin conical sheet". This model interpreted the so-called "sources" as the edges of a hollow emission beam emanating from Io's flux tube crossing the observer's line of sight. From ground observations, Dulk (1967) estimated the half angle of the hollow cone to 79°. Later on, this model has been used to explain the Io-controlled emission (Goldreich & Lynden-Bell, 1969; Thieman & Smith, 1979).

1.2. PRA observations from the Voyager 1 and 2 spacecraft

The two Voyager spacecraft allowed to complete and extend the ground-based observations which are mainly limited to the frequency range above 10 MHz by the terrestrial ionospheric blockage. Dynamic spectra recorded by the Planetary Radio Astronomy experiment (PRA) on board Voyager (Warwick et al., 1977), between 1.3 to 40 MHz, revealed that DAM dynamic spectra consist of nested, curved patterns, the so-called "arcs", in two different frequency ranges: lesser arcs below 15 MHz and greater arcs at higher frequencies. Several authors proposed models, where each arc geometrically results from the rotation of sets of hollow cone beams emanating from a range of frequencies along an activated flux tube threaded by Io (Pearce, 1981; Goldstein & Thieman, 1981; Staelin, 1981). Another explanation was given in terms of diffraction of radio waves by a phase changing plasma structure (Lecacheux et al., 1981). Riddle (1983) could identify the emission which directly comes from the instantaneous Io flux tube with features already noted by Boischot et al (1981). However, Genova & Aubier (1985) found, by examining the distribution of the maximum emission frequency, that most of the Io-dependent emissions should be

Send offprint requests to: A. Lecacheux

emitted well behind the position of the Io satellite (about 70° in longitude) in order to fit the observed maximum frequency with the gyrofrequency available on the Io flux tube (IFT). Most of the authors agree that the half angle of the hollow cone can be estimated from Voyager data as between 70° and 80° (Green, 1984; Genova & Aubier, 1985; Leblanc et al., 1993).

1.3. Correlated observations using space and ground experiments

Simultaneous space and ground observations allowed the study of the beaming of Jovian decametric radiation. Poquerusse and Lecacheux (1978) showed the first direct proof of a narrow beaming of DAM emission, based on simultaneous observations, from the ground (in Nançay) and from space (French-Soviet experiment Stereo-5 aboard Mars 5 spacecraft). During the Jupiter encounter of Voyager, several studies compared ground-based and space observations and enabled the investigation of various effects: the terrestrial ionosphere (Barrow, 1981), the observer's position in longitude (CML) and latitude (D_E) on Jovian arc structures (Barrow et al., 1982), and the solar wind on DAM radiation (Genova et al., 1987).

Due to the excellent sensitivity of the Wind/WAVES experiment the Jovian DAM spectrum can be detected, on a daily basis, in the frequency range from 1 to 14 MHz. The Wind observations, extended towards higher frequencies by adding simultaneous, ground-based data from the Nançay Decameter Array (France), allow to describe in detail the whole Jovian DAM spectrum from 1 to 40 MHz.

In this paper we study two events simultaneously recorded by Wind/WAVES and the Nançay Decameter Array over a large bandwidth (1 to 38 MHz), in order to understand the beam geometry in the frame of available models and usual assumptions on the emission mechanism. In Sect. 1, we report on the characteristics of the used instruments. In Sect. 2, the two selected Io controlled events are described and compared with models. Finally, a discussion on our findings and some still open questions conclude this paper.

2. Equipment

2.1. Wind/WAVES experiment

The Wind spacecraft is a member of the Global Geospace Science program intended to provide characterization of the solar wind upstream from the terrestrial magnetosphere. The satellite was launched at the end of 1994 on a complex trajectory including several lunar swing-by along Earth orbiting elliptical orbits. The spacecraft platform spins at about 20 rotations per minute. Wind includes a radio and plasma wave experiment (WAVES) with the capability of spectral measurements. A complete description of the Wind/WAVES instrument is reported by Bougeret et al. (1995).

WAVES consists in several analyzers, electric and magnetic sensors which allow the study of the electromagnetic spectrum from DC to about 14 MHz. The electrical antenna system is made of two coplanar, orthogonal, 2×50m and 2×7.5m electric dipole antennas in the spin plane, and one rigid, 2×5.3m dipole antenna along the spin-axis. The antenna output voltages of the axial and spinning antennas can be combined in order to synthesize an equivalent, tilted dipole antenna and thus allow the retrieval of the wave polarization and direction of arrival. The RAD2 receiver explores the 1.075 MHz to 13.825 MHz frequency range, over 256 channels every 16 seconds.

The results presented in this work are obtained from this receiver connected to the shorter (2×7.5m) equatorial dipole.

2.2. Nançay decameter array

As reported by Boischot et al. (1980), the main features of the Nançay Decameter Array are a large frequency bandwidth, from 10 to 120 MHz, a high antenna gain of about 25 dB, and a long tracking time, nearly ± 4 hours before and after the transit meridian. The antenna array consists of 144 conical helices, of which one half is right-hand (RH) and one half is left-hand (LH) polarized.

This large array is connected to several receivers whose main objective is the simultaneous analysis of Jovian dynamic spectra in various ranges of time and frequency resolutions. A survey receiver analyzes the outputs of LH and RH sub-arrays over 400 frequencies swept every 0.5 sec between 10 and 40 MHz. This receiver is completed by an acousto-optical spectrograph (AOS) which provides millisecond time resolution in 1000 frequency channels over a bandwidth of 25 MHz. During the common observations with Wind spacecraft we also used a wide-band spectro-polarimeter, which computes in real time the full wave polarisation state (four Stokes parameters), providing the dynamic spectra analysed in this investigation. (For details see Boudjada & Lecacheux, 1991).

2.3. The Wind/Nançay composite dynamic spectra

In the following subsections we analyse two Io-controlled events, each one as a composition of two dynamic spectra recorded at Nançay (in a bandwidth from 40 to 14 MHz) and by the Wind/WAVES experiment (from 14 to 1 MHz). In order to compare sensitivities from ground versus Wind, one has to take into account the different effective area (about 2x4000 m^2 for Nançay and 50 m^2 for the Wind antenna) and the galactic background noise (about 10^7 K at 3 MHz and 10^4 K at 30 MHz). This implies that the Nançay instrument is much more sensitive than Wind, by a factor of about 100. Therefore we proceed by three steps to standardize both observations. The first step provides a correction of the Wind data from modulation effects due to the satellite spin. The second step equalizes the apparent contrasts of Jovian emission recorded by the Wind spacecraft; therefore the gray shading scale (increasing in intensity from white to black) used in the figures has no quantitative meaning . In the last step both data sets have been resampled, in time and frequency, in order to take into account the different spectrometer capabilities.

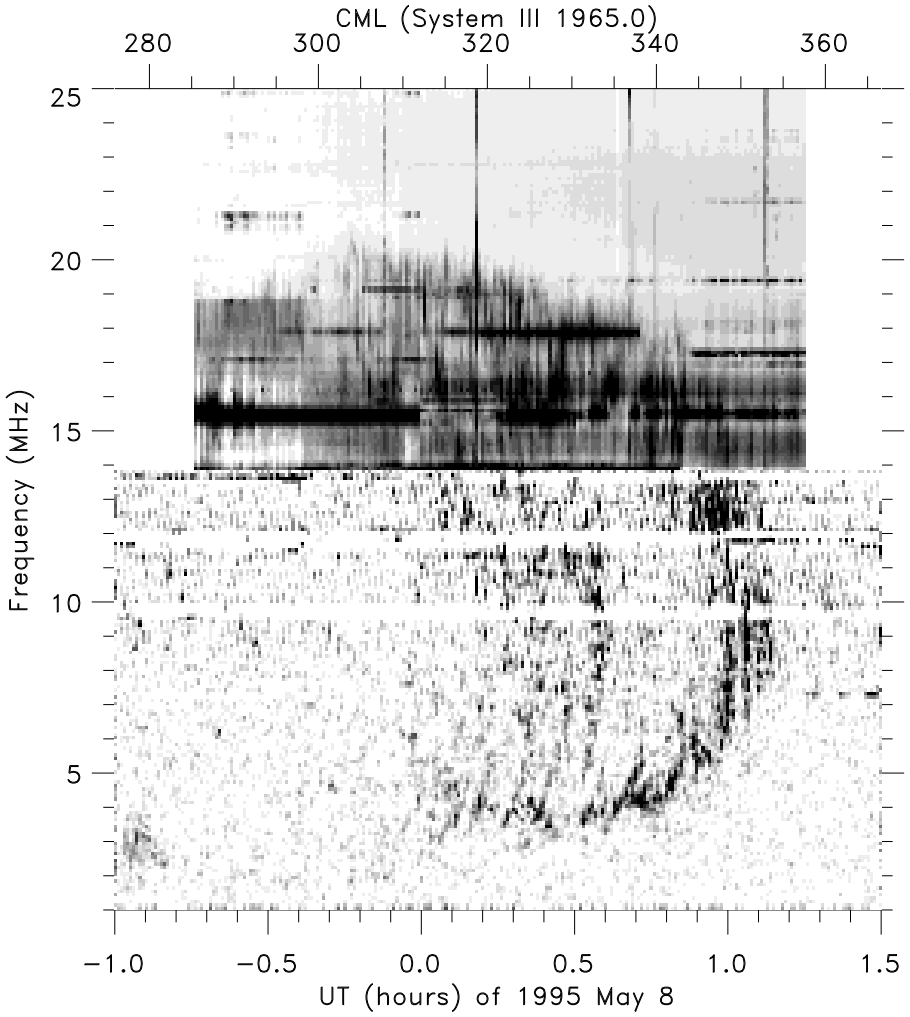

Fig. 1. Dynamic spectrum of a Jovian decametric emission, recorded on 1995, May 8^{th}, and associated with Io-C configuration (at 01:00 UT, CML=348° and Φ_{Io}=258°). The complete arc-shaped pattern is a composition of the Nançay and Wind/WAVES spectral measurements, from 25 to 13.5 MHz and 13.5 to 1 MHz, respectively. According to Nançay polarisation determination the event is 100% left-hand polarized. Dark or white horizontal streaks are due to RF interferences.

3. Observations

3.1. The Io-C controlled event May 8^{th}, 1995

As shown in Fig. 1 the Io C event appears as an arc composed of two parts, beginning nearly at the same time, at 23:30 UT (on May 7^{th}) and 00:10 UT, at 20 and 6 MHz respectively. Both components meet each other at the vertex late point, corresponding to the end of emission, one hour after the beginning, and at a frequency of 8 MHz. From the Nançay spectropolarimeter, this arc is found to be left-hand polarized as documented by other studies (Dulk et al., 1994; Leblanc et al., 1994). From CML and Io phase values this event belongs to the Io-C region. Such an arc was already reported by Boischot et al. (1981) using Voyager data where it appeared as very irregular arc (see Fig. 4a of Boischot et al.,1981). One Voyager radio discoveries was the detailed structure within an arc; this is shown in Fig. 1 in particular below 8 MHz where one can distinguish "small" arcs included within the main arc. More details about this type of fine structure was reported by Wilkinson (1989).

The ground observations showed that the Io-C arc is often associated with two others recorded at low frequency, below 24 MHz (see Fig. 6a-b of Boudjada & Genova, 1991; Fig3a-h of Boudjada et al., 1995).

3.2. The Io-controlled B/D event May 8/9^{th}, 1995

About one day later, the event shown in Fig. 2 was recorded during three hours. In this period the central meridian longitude changes by about 100° and the Io-phase by nearly 25°. Both polarizations are observed, right-hand (RH) and left-hand (LH), assuming an origin from both Northern and Southern hemispheres; this is in agreement with an extraordinary mode emission.

The earlier observed emission belongs to Io-D controlled region. It is observed in the frequency range from 23.5 to 1.5 MHz, with a left-hand circular polarization. From Nançay (above 20 MHz) the radiation is measured as 100% LH polarized. We can distinguish two regions in the arc shape of this Io-D event. The part above 14 MHz appears as slowly drifting narrow band increasing during 2.5 hours from 16 MHz to 23.5 MHz. This behavior is typical for Io-D events as reported by several authors using Voyager data (see Fig. 3e and 4b of Boischot et al., 1981; Fig. 16 of Leblanc, 1981, and Fig. 3 of Genova & Aubier,

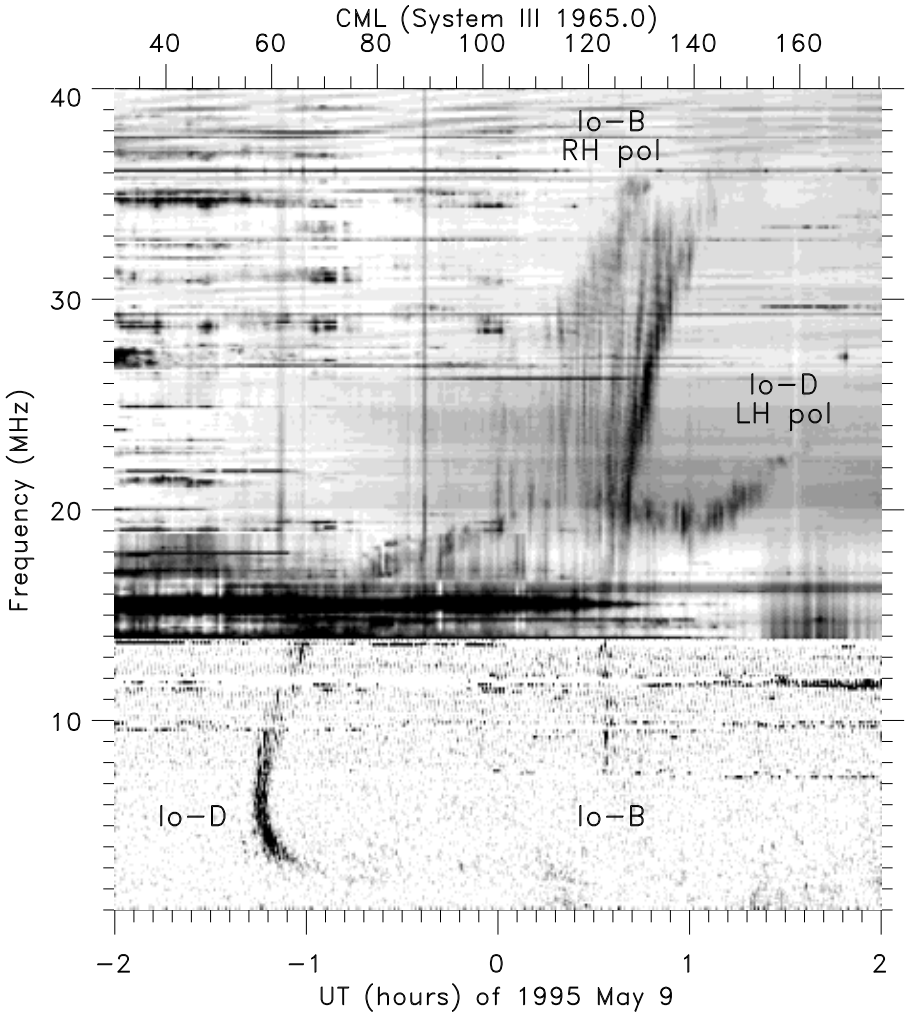

Fig. 2. Dynamic spectrum of the event of 1995, May 8/9th, displaying the complete beam pattern of the Io flux tube radiation. Two Io-controlled arc-shaped patterns are recorded, Io-B and Io-D, in opposite sense of circular polarizations. Both radiations are observed together during more than one hour, each emanating from different hemispheres. As in the previous event, the dynamic spectrum is the composition of two observations, from Nançay and Wind/WAVES.

1985), and from ground observations (see Fig. 4 of Boudjada & Genova, 1991). The earlier part of the Io-D emission, in front of the previous one, appears as narrow band, too, but with an arc shape. This arc presents an asymmetric shape with components simultaneously observed during one hour, in frequency range from 1.5 to 14 MHz. The change in the drift sign (vertex-point) is recorded at the beginning of the emission (around 22:45 UT on May 8th, 1995) at a frequency of about 6 MHz. The entire Io-D pattern, such as observed here (Fig. 2), was never reported before in the literature.

Nearly one hour after the start of the Io-D event, the typical pattern of the Io-controlled B event (Io-B) was recorded. This event was reported by several authors (see Figs. 2 and 3 of Dulk, 1965; Fig.4b of Boischot et al., 1981; Fig. 1a of Lecacheux et al., 1991). The Io-B radiation is the most broadband Io-controlled emission which extends, in the case of Fig. 2, from 38 MHz (on the original data) down to 8 MHz, over a time span of 2 hours. From the Nançay spectropolarimeter, we find that the emission is 100% RH polarized, as typically are those of Io-B region, in accordance with a previous study (Lecacheux et al., 1991). Therefore, this Io-B/D event likely displays the complete pattern of the Jovian Io-controlled radiation activated both in Northern and Southern hemispheres along, or close of, the Io flux tube.

4. Analysis of emission beaming geometry

In the following, we assume that the source region is located along the Io flux tube, at an altitude where the electron gyrofrequency is nearly equal to the emitted frequency. To estimate the angle γ between the line, parallel to the local magnetic field and oriented outward, and the direction of the observer (e.g. the Wind spacecraft or the Earth), we use the O6 model. This model proposed by Connerney (1992) can be considered as the most appropriate description of the magnetic field of Jupiter close to the surface of the planet, for computing the half angle of the hollow cone emission. Indeed, Connerney (1992) estimated the uncertainty of this model to better than 10° in direction and within 3 Gauss (i.e. about 10 MHz) of the actual intensity. This assessment seems to be confirmed by the analysis of recent images of the Jovian aurorae, taken at UV and IR wavelengths (Baron et al., 1996; Connerney et al., 1996; Clarke et al., 1995; Gérard et al., 1994), on which the observed auroral oval is consistent with the modelled one.

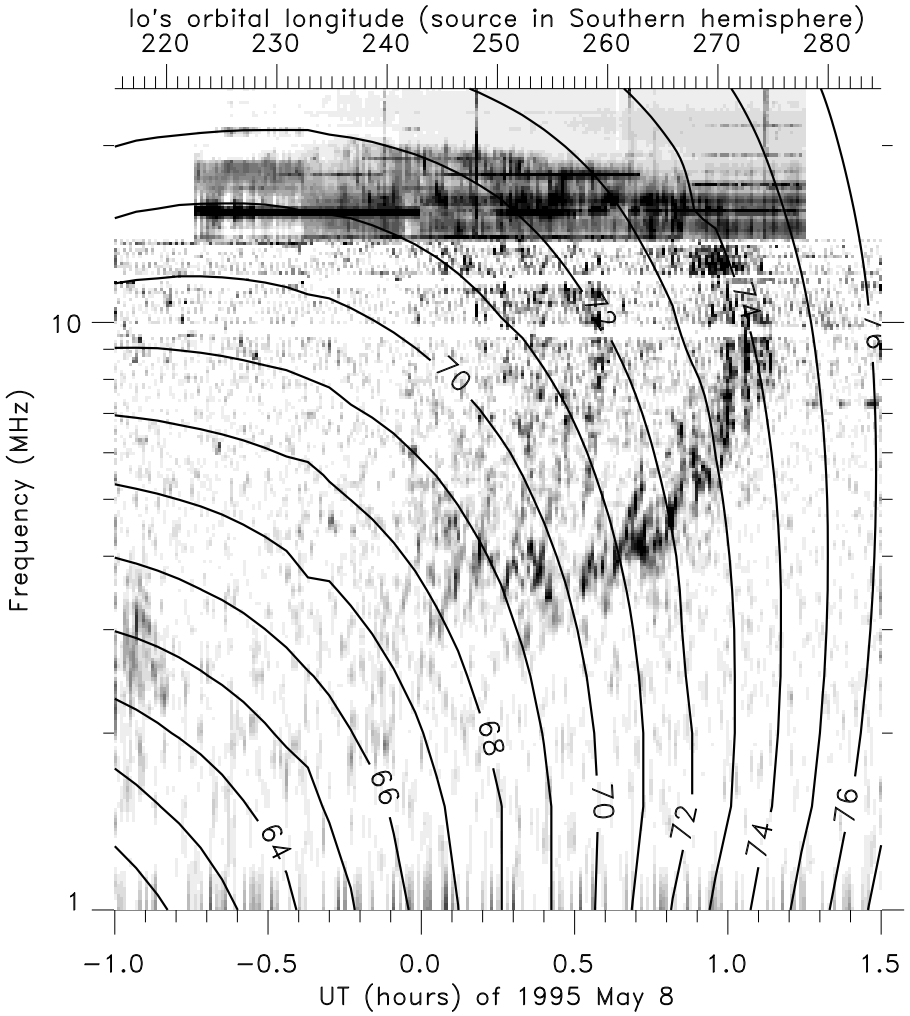

Fig. 3. The calculated isocontour of the apparent emission angle, deduced from a hollow conical radiation beam, is superposed to the dynamic spectrum in Fig. 1 It is obviously impossible to "fit" the observed main arc by any of the modelled contours, in particular at frequencies lower than 8 MHz.

In the following analysis we will compare the shape of the arc structure with the calculated γ change in function of the time and the frequency. For this comparison, the arc structure is identified with the emission cone as represented by γ. Indeed, if we could neglect reflection or refraction effects, the angle γ would merely be equal to the half opening angle of the radiation beam.

In the case of the Io-C event (Sect. 4.1), Fig. 3 displays the isocontour of the computed angle γ overlayed on the observed dynamic spectrum. As described in the previous section this event is totally left-hand polarized, thus we begin to examine the isocontour of γ for a radiation coming from the Southern hemisphere. Obviously, the predicted shapes of the curved lines, resulting from different values of the beam opening angle, does not correspond to the observed arc shapes, in particular at frequencies lower than 8 MHz. One gets only some resemblance with the sense of curvature of the most intense arc feature, within the middle frequency range. While the discrepancy can be understood at higher frequencies - since the influence of the unknown, high-order, multipolar terms of the Jovian magnetic field would be larger -, the shape of the main arc at lower frequency, is much more difficult to understand in terms of observer line of sight intersecting the conical sheet of the emission beam. On the other hand, if we assume that the radiation comes from the Northern hemisphere, isocontours present opposite slopes and even more different curvatures than those observed.

A secondary arc sub-structure can be discerned on the dynamic spectrum (especially near 0.5 UT and inside the main arc); this sub-structure was already discussed by Wilkinson (1989), who suggested that it might directly trace the emission beam, while the main arc feature would rather be the consequence of an additional process leading to an enhancement of the emission intensity. Wilkinson proposed the encounter of the IFT with a discrete, extended in longitude, active radio source surrounding the interaction region. It is interesting to note that the arc sub-structure is somewhat closer to the form of the γ isocontour grid (Fig. 4), if one assumes that the active flux tube lies about 1 hour, or 28°, ahead the IFT.

In the case of the Io-B/D event on May 8/9th, the emission is assumed to come from both hemispheres in opposite circular polarizations. As in the previous event, the γ isocontour is superimposed on the dynamic spectrum (Fig. 5 and 6). The contour corresponding to the geometrical horizon is also displayed (thicker, dark line): the horizon is defined as the plane tangent

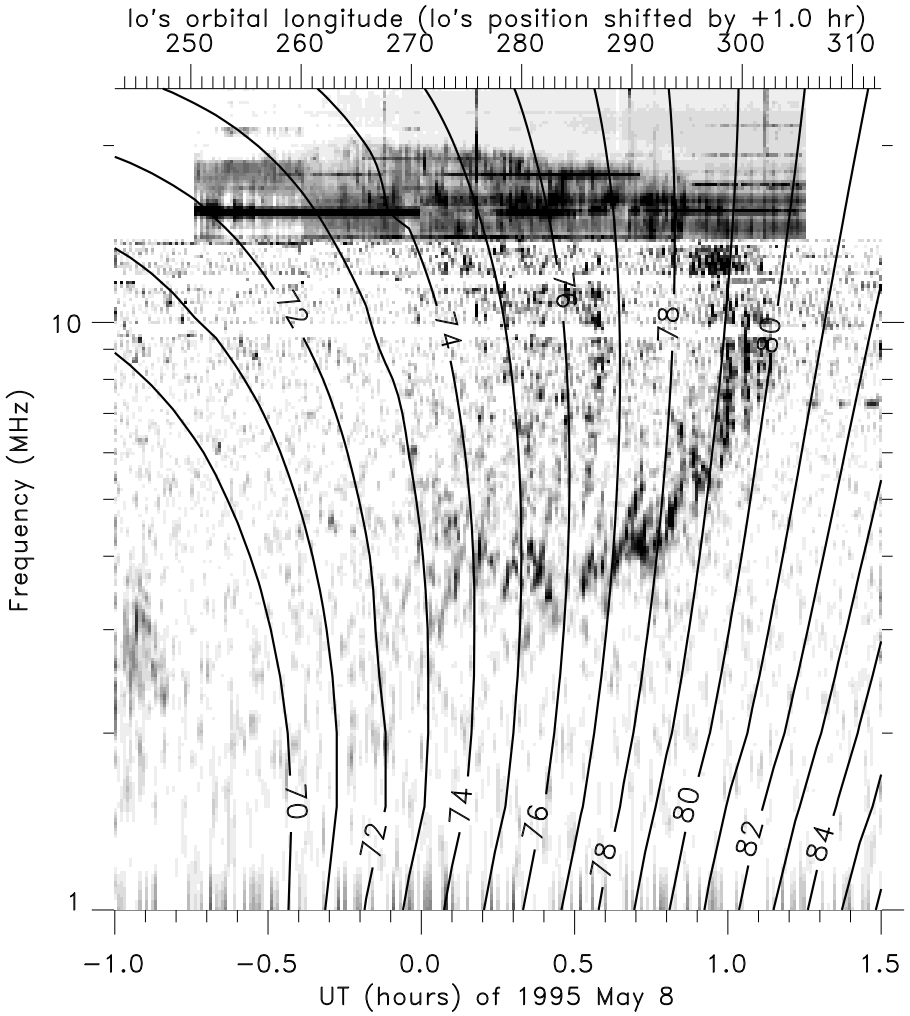

Fig. 4. Same as Fig. 3 but arbitrarily shifting Io's longitude by +1.0 hr or 28°, in order to simulate source offset from instantaneous IFT or magnetic field distorsion.

to the refractive index surface at the source or, quite closely, to the plane orthogonal to the gradient of the magnetic field intensity. It must be noticed that the horizon may substantially differs from the plane perpendicular to the magnetic field vector, even in the case of a magnetic dipolar field: the difference may be quite enlarged by the existence of high-order multipolar terms.

In both polarizations, the computation shows, as expected, that the emission is observed when the observer is just above the geometrical horizon (thick line on the figures): along the whole event duration γ remains acute but very close to 90° . Since the DAM radiation is thought to be emitted in the X-mode, the radiation has therefore propagated near grazing incidence, just above the reflecting, X-mode cut-off surface, before reaching the observer. In the lowest frequency range, below 20 and 6 MHz for Io-B and D respectively, the magnetic field model is in agreement with a beam aperture of about 87°. Conversely, at higher frequencies, isocontours no longer fit with the shape of the observed arcs.

Consistent results at low frequencies are anticipated because of the smaller contribution of the non dipolar terms and the expected small refraction effect at far distance from Jupiter. But close to the source region, where higher frequencies are emitted, the refraction effect might be important. This effect can be checked by computing, for each frequency, the source altitude above the cloud level. One finds that the apparent opening angle of the emission beam starts to decrease, by more than 0°.5 at about 18 MHz (resp. 6 MHz) when the source altitude reaches 0.2 R_J (resp. 0.6 R_J) in the Northern (resp. Southern) hemisphere. The emission cone thus closes in when the altitude decreases, as expected from a beam pattern mainly governed by wave refraction above a reflecting surface. Since refraction effects are proportional to the square of the frequency we can deduce from the previous numbers that the electron density should be in a ratio of 9:1 when altitudes above the cloud level change from 0.6 to 0.2 R_j. This implies a scale height of about 1200 km for the topside ionosphere electron density. On the other hand the magnitude of the observed angular deviation from the nominal emission angle $\gamma = 87°$ reaches about 3° at 30 MHz and at very low altitude. Application of Snell's law then gives a crude estimate of 3 $10^4 cm^{-3}$ for the plasma density at the top of the ionosphere in the vicinity of the radio source. These numbers are in reasonable agreement with the measured properties of the Jovian ionosphere (Strobel & Atreya, 1983).

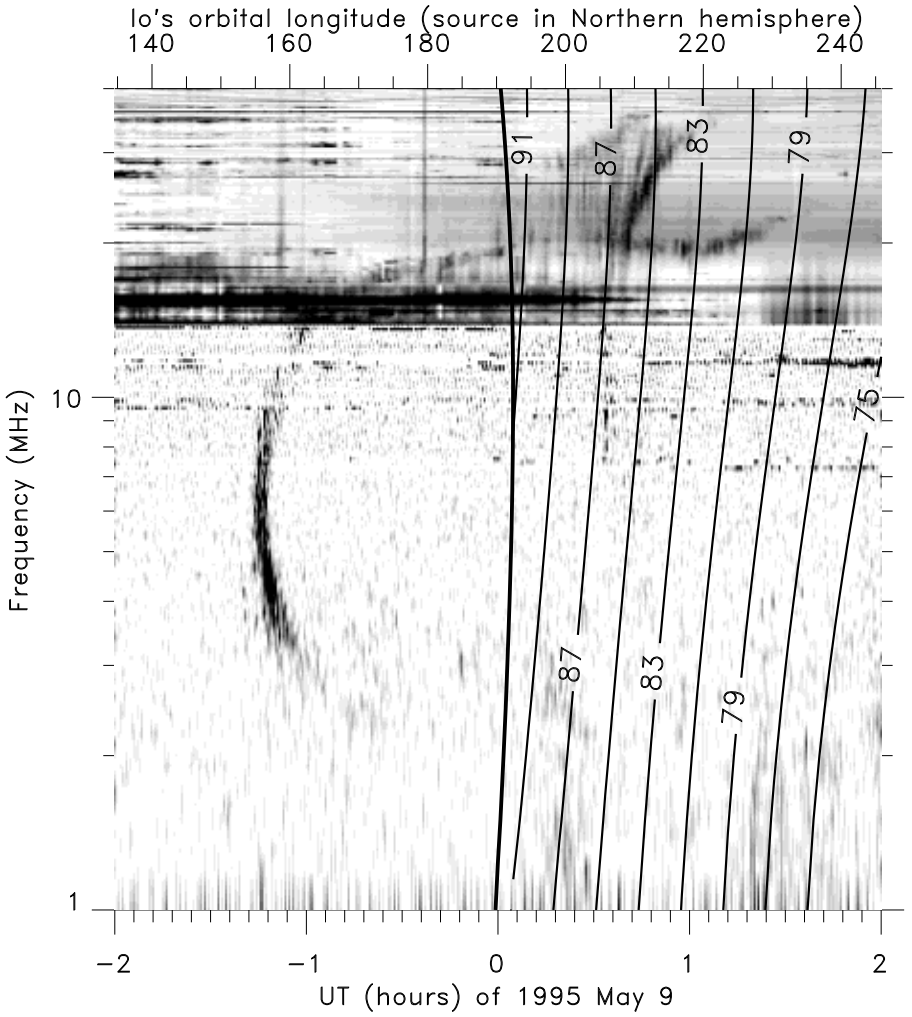

Fig. 5. Same as Fig. 3 but for the Io-B (RH polarized, or Northern hemisphere) emission. The dark, thicker contour line represents the geometrical horizon at the source; the observed dynamic spectrum begins when the observing direction rises above this plane.

Above 20 MHz, the left-hand polarized component is far from being arc-shaped and previous estimations are no longer possible: maybe not coincidental is the similar change (see Fig. 6), in the same range of gyrofrequencies, of the modelled shape of the isocontour lines due to the quadrupolar and octupolar components of the Southern magnetic field.

5. Summary and conclusion

In this work we analyzed two examples of composite dynamic spectra derived from data provided by the Wind/WAVES radioastronomy experiment and by the Nançay Decameter Array (France). This allows us to produce complete dynamic spectra of DAM emission, up to 40 MHz, and to compare the shape of the arcs with the emission beaming geometry.

Both analyzed events are typical of Io-controlled DAM emission events, that one can assume to be directly produced by moving electrons along the instantaneous magnetic flux tube threaded by Io. Using an appropriate Jovian magnetic field model, we have compared the observed spectral shapes with the apparent beaming angle γ defined as the angle between the direction of the magnetic field vector in the source region, and the direction of the observer.

Our main findings are the following:

a) For both Io-C and Io-B/D events, significant discrepancies are found between the calculated angle and the observed shapes of the main arc-shaped structures.

b) The discrepancies occur at lower as well as at higher frequencies; therefore they cannot be explained merely by an insufficient knowledge of the magnetic field topology at the source, which is closely dipolar in regions where the gyrofrequency is only a few MHz. Other explanations must be invoked, as beaming angle changes with the frequency; distorsions of the static magnetic field lines when the Io perturbation passes through; source interaction model more complex than anticipated; or refraction effects in the source region.

c) In the case of the Io-controlled B/D event, we find that the radiation might be originally emitted quasi-perpendicularly to the magnetic field in the source. In the higher frequencies part of the spectrum, the disagreement between the calculated beaming geometry and the observations could be explained by refraction of the radio waves at grazing incidence on the "radio horizon" above the planetary limb. In making the plausible as-

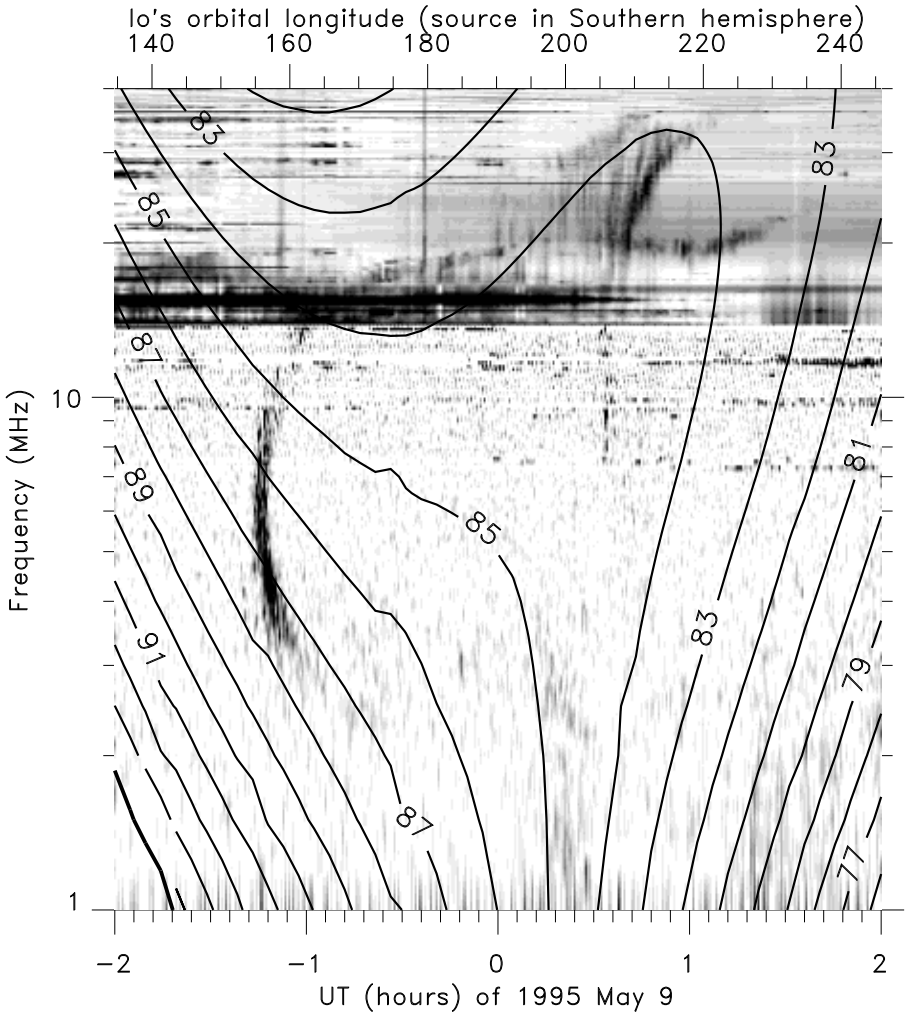

Fig. 6. Same as Fig. 5 but for the Io-D (LH polarized, or Southern hemisphere) emission. Note the magnetic anomaly (change in curvature of the iso-contour lines) and the (maybe coincidental) distortion of the arc shape emission.

sumption that both radiations, Io-B and Io-D, likely belong to the same instantaneous IFT and that each one is emitted from opposite hemispheres, we found that the magnitude of the necessary refraction effect is consistent with ionospheric parameters deduced from radio link occultation experiments on Pioneer and Voyager spacecraft (Strobel & Atreya, 1983).

The quite large differences between the dynamic spectra displayed by the Northern and Southern radiations would be due to the combined magnetic field asymmetry (field lines not contained in meridian planes) and small refraction effects in the low altitude ambient plasma. In this scenario, the deduced emission angle is 87° and the thickness of the beam, deduced from the duration of the most intense, arc shaped features at a given frequency, is much less than 1°. It is worth noticing that the strongest emission intensity is only observed at the interior edge of the refracted emission beam and, therefore, might correspond to an intensity enhancement due to wave diffraction on an edge caustics (Lecacheux et al., 1981). This is also suggested by the presence of fine structures along and inside the intensity enhancement.

d) The Io-C controlled event is more difficult to interpret. We find that neither calculated arc shapes nor values of opening angle are consistent with the observed dynamic spectrum.

The discrepancy could be due to some of our assumptions in computing the emission beam geometry. In particular, the assumption that the radiation is directly produced on the IFT might be untrue. However, Genova & Aubier (1985) demonstrated, from Voyager data, that the Io-C radiation is likely to be emitted along the Io field line. Later on, Connerney et al.(1993) showed that some Jovian Southern aurorae are located very close to the position of the calculated IFT footprint and occur at the time of the Io-C configuration (see Fig. 2b of Connerney et al., 1993).

On the other hand, we did not yet take into account any possible dependance of the emission angle on the frequency, due to the generation mechanism and to the varying magnetoplasma conditions along the active field line. Such a dependance can directly be extracted from the dynamic spectrum of each of the three main arcs that we have observed (one on May 8 and two on May 9) and should follow some generic γ(f) function. Unfortunately, each of the three obtained functions is quite specific of the observed event and does not appear to contain relevant information of this kind.

Finally, wave propagation effects, occuring close or inside the radio source, seem to us the more satisfying explanation. Following the generally admitted maser cyclotron scenario, the DAM radiation is emitted nearly perpendicular to the magnetic field, leading to a hollow cone emission pattern, but is also produced at low altitude above a reflecting layer (stop zone of the propagating X-mode). In the case of the Io controlled DAM radiation at Jupiter, the ambient magnetic field topology is complex and the source follows the motion of Io; therefore, the source altitude, the principal curvatures of the reflecting surface as well as the orientation of the radiated beam with respect to this surface, are continuously changing functions of the active field line position. In some cases, the emission beam can even be directed towards the reflecting surface and then must suffer substantial refraction, implying different kinds of intensity modulations like edge effects or interfering phase paths. The resulting radiation pattern can therefore be quite distorted with respect to the expected one.

In summary, it appears from our analysis that any crude interpretation of the observed "arcs" curvature, by the change of time and frequency of the emitting field line geometry, is insufficient by itself to account for DAM, arc-shaped patterns. In both events described in our study, which are representative of Io-controlled radiation, we must introduce refraction effects to explain the discrepancy between observations and beaming geometry. These effects likely take place in the source region, mainly at higher frequencies, as expected. But refraction effects are also needed at frequencies below 3 MHz (Fig. 1) and might occur in the Io plasma torus. More investigations should be made to analyse this possibility.

References

Baron, R., T. Owen, J.E.P. Connerney, T. Satoh, and J. Harrington 1996, Icarus, 120, 437

Barrow, C.H. 1981, A&A, 101, 142

Barrow, C.H., A. Lecacheux, and Y. Leblanc 1982, A&A, 106, 94

Bigg, E.K. 1964, Nat, 203, 1008

Boischot, A., C. Rosolen, M.G. Aubier, G. Daigne, F. Genova, Y. Leblanc, A. Lecacheux, J. de la Noë, and B. Möller-Pedersen 1980, Icarus, 43, 399

Boischot, A., A. Lecacheux, M.L. Kaiser, M.D. Desch, J.K. Alexander, and J.W. Warwick 1981, JGR, 86, 8213

Boudjada, M.Y. and A. Lecacheux 1991, A&A, 247, 235

Boudjada, M.Y., and F. Genova 1991, A&AS, 91, 453

Boudjada, M.Y., H.O. Rucker, and P.H. Ladreiter 1995, A&A, 303, 255

Bougeret, J.L., M.L. Kaiser, P.J. Kellogg, R. Manning, K. Goetz, S.J. Monson, N. Monge, L. Friel, C.A. Meetre, C. Perche, L. Sitruk, S. Hoang 1995, Space Sci. Rev., 71, 231

Burke, B.F., and K.L. Franklin 1955, JGR, 60, 213

Clarke, J.T., R. Prangé, G.E. Ballester, J. Trauger, R. Evans, D. Rego, K. Stapelfeldt, W. Ip, J.C. Gérard, H. Hammel, M. Ballav, L. Ben Jaffel, J.L. Bertaux, D. Crisp, C. Emerich, W. Harris, M. Horanyi, S. Miller, A. Storrs, and H. Weaver 1995, Sci, 267, 1302

Connerney, J.E.P. 1992, Planetary Radio Emissions III, Austrian Academy of Sciences Press, Vienna

Connerney, J.E.P., R. Baron, T. Satoh, and T. Owen 1993, Sci, 262, 1035

Connerney, J.E.P., T. Satoh, and R.L. Baron 1996, Icarus, 122, 24

Dulk, G.A. 1965, Ph. D. Thesis, Colorado Univers., Boulder

Dulk, G.A. 1967, Icarus, 7, 173

Dulk, G.A., Y. Leblanc, and A. Lecacheux 1994, A&A, 286, 683

Genova, F., and M.G. Aubier 1985, A&A, 150, 139

Genova, F., P. Zarka, and C.H. Barrow 1987, A&A, 182, 159

Gérard, J.C., V. Dols, R. Prangé, and F. Paresce 1994, Planet Space Sci., 42, 905

Goldreich, P., and D. Lynden-Bell 1969, ApJ, 156, 59

Goldstein, M.L., and J.R. Thieman 1981, JGR, 86, 8569

Green, J.L. 1984, Radio Science, 19, 2

Leblanc, Y. 1981, JGR, 86, 8564

Leblanc, Y., F. Bagenal, and G.A. Dulk 1993, A&A, 276, 603

Leblanc, Y., G.A. Dulk, and F. Bagenal 1994, A&A, 290, 660

Lecacheux, A., N. Meyer-Vernet, and G. Daigne 1981, A&A, 94, L9

Lecacheux, A., A. Boischot, M.Y. Boudjada, and G.A. Dulk 1991, A&A, 251, 339

Pearce, J.B. 1981, JGR, 86, 8579

Poquerusse, M., and A. Lecacheux 1978, Nat, 275, 111

Riddle, A.C. 1983, JGR, 88, 455

Staelin, D.H. 1981, JGR, 86, 8581

Strobel, D.F., and S.K. Atreya 1983, Physics of the Jovian Magnetosphere, Cambridge University Press, New York

Thieman, J.R. and A.G. Smith 1979, JGR, 84, 2666

Warwick, J.W., J.B. Pearce, R.G. Peltzer, and A.C. Riddle 1977, Space Sci. Rev., 21, 309

Wilkinson, M.H. 1989, JGR, 94, 11777

This article was processed by the author using Springer-Verlag LaTeX A&A style file *L-AA* version 3.